Effects of laser bandwidth on OPE in a modern lithography tool.

Kevin Huggins[*a], Toki Tsuyoshi[b], Meng Ong[c], Robert Rafac[d], Christopher Treadway[a], Devashish Choudhary[a], Takehito Kudo[b], Shigeru Hirukawa[b], Stephen P. Renwick[c], and Nigel R. Farrar[d]
[a]Intel Corp., 5200 NE Elam Young Parkway, Hillsboro, OR 97124;
[b]Nikon Corporation, 201-9 Oaza-Mizugahara, Kumagaya, Saitama 360-8559 Japan;
[c]Nikon Precision, Inc., 1399 Shoreway Rd., Belmont, CA 94002;
[d]Cymer Inc., 17075 Thornmint Court., San Diego, CA 92127.

ABSTRACT

The OPE signature of a lithographic stepper or scanner has become a very important characteristic of the tool, as it determines the OPC correction to be applied to reticles exposed on that tool. The signature depends on a variety of detailed information about the scanner lens and illuminator, which in turn depend on the characteristics of the illumination light from the laser.

Specifically, changes in the laser bandwidth should impact OPE as the lens exhibits some chromatic aberration. Tool-to-tool differences and time fluctuation of the laser bandwidth could cause variations in OPE tool matching and stability.

To assess this, a detailed study of laser bandwidth effects on OPE was performed. A sensitive spectrometer was connected to a litho laser, allowing careful measurements of both the FWHM and E_{95} parameters of the laser spectral profile.

Lithographic modeling using the chromatic response of the lens was run in order to predict effects. Exposures of CD through pitch were made to test the modeling. Finally, the bandwidth data was correlated with litho sensitivity to create a "bandwidth effect", put in context with the other common scanner parameters affecting OPE.

Keywords: laser, bandwidth, chromatic aberration, FWHM, E95, OPE, OPC

1 INTRODUCTION.

With optical proximity correction (OPC) playing such a large role in modern low-k_1 processes, the through-pitch CD performance of a lithographic scanner is a very important criterion. Due to the optical-proximity effect (OPE), CD of dense lines is inevitably different from that of isolated lines. This behavior, characteristic of a particular illumination pattern, lens NA, feature type, and process, is frequently captured in a single signature referred to as an OPE curve or a coherence curve. A sample of such a curve is shown in Figure 1.

Several important parameters of a lithographic scanner can affect OPE and thus affect OPC. Since OPC is such a complicated effort, modern lithographers need to concern themselves with the stability of a particular OPC solution when it is applied to reticles exposed on different litho tools or on the same tool at different times. Thus, the OPE drivers on the scanner need to be understood in order to assess how precisely the scanner needs to be characterized and how tightly it must be controlled.

Previous work[1] has investigated the effects of focus, dose, lens NA, illuminator partial coherence, and lens aberrations, and has ranked them in order of importance (roughly, the same order given here). One item that has been neglected so far is a key parameter of the illumination light entering the scanner--the bandwidth of the laser light source.

* kevin.e.huggins@intel.com, phone 503-613-8527.

Optical Microlithography XIX, edited by Donis G. Flagello, Proc. of SPIE Vol. 6154
61540Z, (2006) · 0277-786X/06/$15 · doi: 10.1117/12.656816

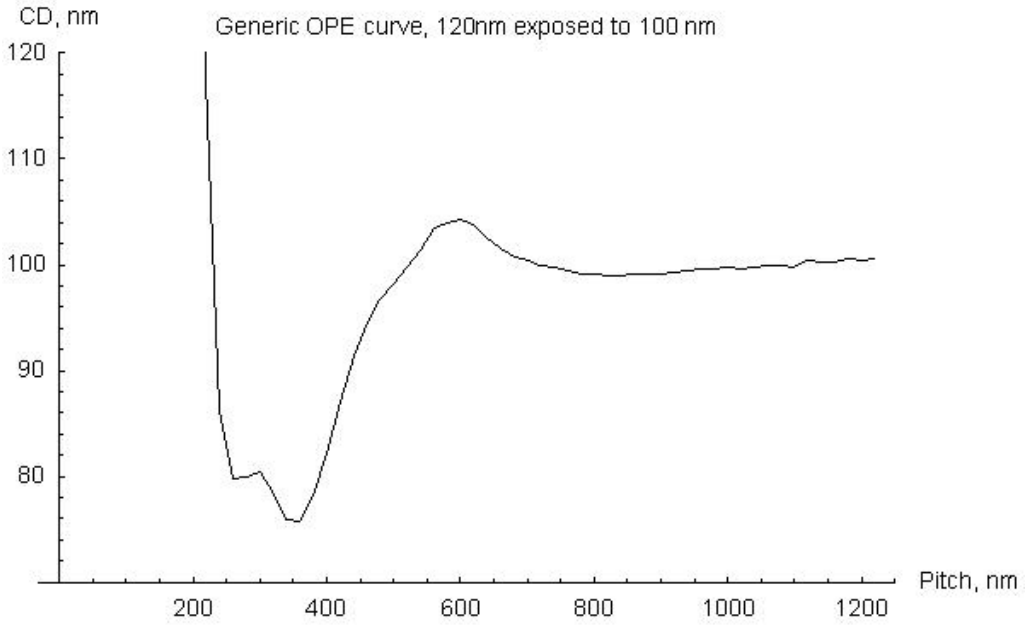

Figure 1.
A sample OPE curve, showing CD dependence through pitch for constant-width features.

Although it is difficult to assess, one can certainly expect there will be some effect of bandwidth on OPE. All lithographic lenses are made of glass and crystalline materials (in the case of ArF optics, fused silica and CaF_2), which are dispersive, in that their index of refraction depends on the illumination laser wavelength. Good lens design helps to mitigate this effect, but every lens will have not only a set of aberrations, but also a characteristic *change* in aberrations as the incident wavelength is varied. Lasers, on the other hand, are not truly monochromatic but instead have a certain center wavelength and bandwidth, which describes the distribution of wavelengths around the center value. The combination of these effects contributes to the performance of the tool both at any instant and over time, since bandwidth is not perfectly stable.

We have studied this effect both in modeling and in experiment. In modeling, known chromatic response of the lens was coupled with known bandwidth of the laser in order to calculate expected changes in OPE. In the experiment, laser parameters such as the fluorine concentration in the gas mixture or trigger timing were varied, the resulting bandwidth was measured with an on-board spectrum analyzer which can monitor both FWHM and E_{95}, and the effect on measured OPE was observed.

2 THEORY AND MODELING

Prior to executing the OPE-vs-bandwidth experiments, lithographic modeling was run to predict the effects. To understand the reasons behind OPE shifts with laser bandwidth, it is necessary to grasp both the response of a lithographic lens to polychromatic illumination and the metrics for laser bandwidth. These subjects have been discussed in detail in the past, so a brief overview is given.

A sample laser spectral shape is shown in Figure 2. As is typical, it is neither a pure Gaussian nor a pure Lorentzian profile. The lens in the exposure tool receives a superposition of light waves at different wavelengths. Since the lens aberration set depends on wavelength, its reaction to this input spectrum will be to project a superposition of images that are formed with slightly different aberrations. Typically, the predominant aberration shift will be a defocus, followed by spherical aberration and coma[2]. Wider bandwidth therefore tends to reduce contrast of the aerial image projected by the lens. Since the illumination pupil fill is unaffected by wavelength shifts, and lateral chromatic aberration effects tend to be smaller, this lens-dependent effect is the primary means for a bandwidth shift to affect image contrast.

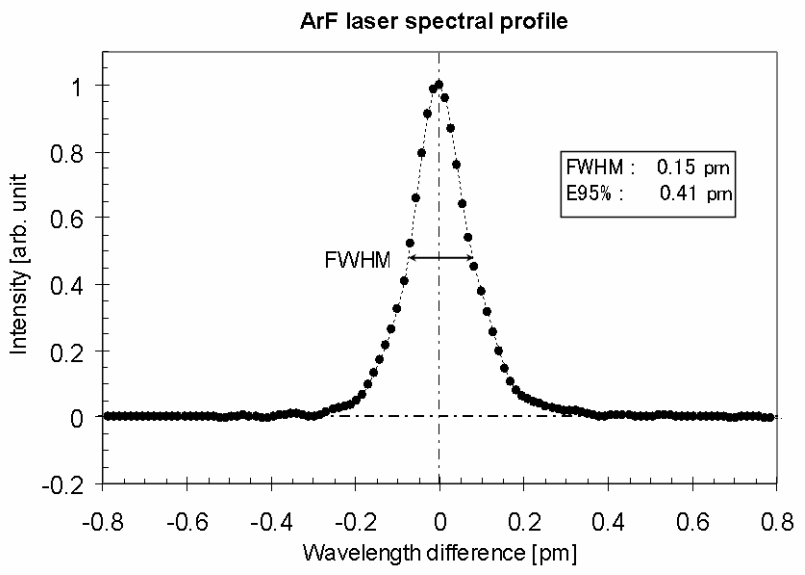

Figure 2.
Sample spectral profile of an ArF litho laser.

In this study, the primary interest is the response of the lens (and thus the imaging) to a *change* in bandwidth, not to the absolute value, particularly to characterize changes in OPE as bandwidth is modulated. It is worth noting that an attempt to measure aberration shifts interferometrically as bandwidth is adjusted will fail, as the measuring instrument will respond to the average wavelength just as the imaging will. For that reason, aberration measurements are not reported in this study. Of course, one may alter the laser center wavelength and measure aberration shifts, as has been done with earlier lithographic tools[3], but there is no reason to do that here. The most important chromatic lens aberration responses, listed above, are available and used in the modeling.

The model also used a characteristic full spectral profile of the laser, but it is useful to present the response with a single figure of merit for the spectral profile. Two metrics of the profile are widely used: the full width at half-max (FWHM), and the E_{95} parameter [4]. The FWHM is shown on the plot, while E_{95} is defined as the width that contains 95% of the integrated spectral intensity. No single number can capture the entire characteristic of the spectrum, but from a lens designer point of view the E_{95} metric is in general better than the FWHM metric for tracking lens response. Unfortunately, E_{95} is also much more difficult to measure than the FWHM, in part due to its sensitivity to background light so, until recently, laser vendors have tended to include the FWHM (or an approximation to it) in on-board metrology and diagnostics. The modeling, of course, has no such restriction. The entire spectrum is included and the results tracked with the E_{95} parameter are reported.

Aerial-image modeling was run using the laser and lens information discussed here as well as other parameters listed in Table 1. Results for the 80-nm lines are shown in Figure 3. In the graph on the left, a clear contrast loss is observed everywhere throughout the modeled pitch range as E_{95} is increased.

Table 1.
Parameters used in aerial-image model.

Parameter	Value
Tool	
LNA	Greater than 0.75
Illum type	Annular, with profile resembling a Nikon illuminator profile.
Outer sigma	Greater than 0.70
Annular ratio	0.50
Lens aberrations	Varied according to known sensitivity to wavelength.
Laser spectrum	Experimental spectrum used, with images integrated over it.
Bandwidths used	E_{95} = 0.27, 0.31, 0.38, and 0.59 pm.
Mask	
Type	EPSM
Feature size	80, 90, 100, 110, 130 nm
Pitches	160 to 2100 nm.
Metrology	Measure width of aerial image at constant threshold value, with threshold set at the isolated line.
Resist stack	None: aerial-image model only.

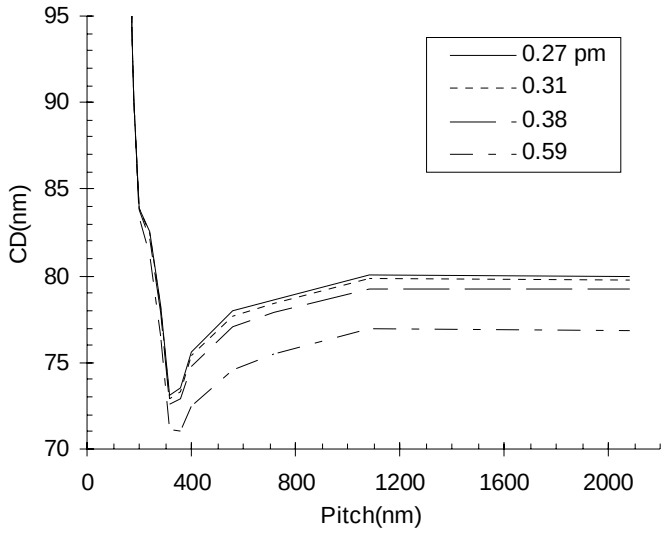

Figure 3.
Aerial-image modeling of OPE of 80-nm lines as laser bandwidth is changed.

A better understanding of the bandwidth effect is obtained by looking at the CD sensitivity to bandwidth change. As a function of pitch *p*, this is given by:

$$S(p) \equiv \frac{dCD(p)(\text{nm})}{dE_{95}(\text{pm})}. \quad (1)$$

This sensitivity parameter was calculated by, at each pitch, using all four values of E_{95}, all four modeled CD values, and evaluating the slope of a line fitted through them (the CD variation is expected to be nonlinear with respect to E_{95}, but in the model and the data the non-linearity was negligible). This quantity is plotted in Figure 4.

The modeled results agree with the physical explanation mentioned earlier. As bandwidth is changed, the primary lens effect is a defocus. Dense lines tend to have greater depth of focus than isolated lines, so their sensitivity to the bandwidth change is much less than that of the isolated lines. We will compare this to experimental results in Section 4.

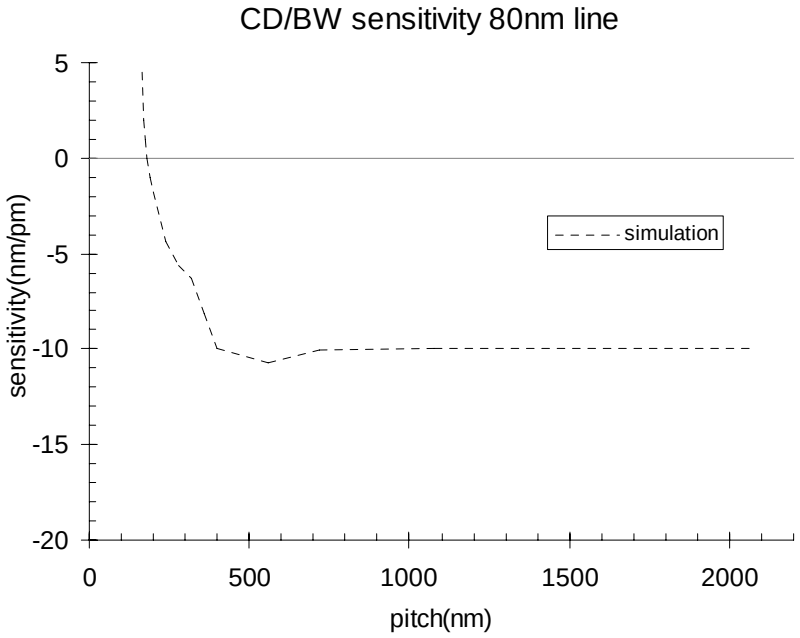

Figure 4.
The modeled CD sensitivity to change in E_{95} bandwidth (defined in Eq. (1) in the text).

3 EXPERIMENTAL CONTROL OF LASER BANDWIDTH.

In this experiment, a Nikon S307 scanner integrated with a Cymer XLA 140 193 nm, ArF-excimer MOPA (master oscillator/power amplifier) light source was used, as shown schematically in Figure 5. For the purposes of this experiment, the bandwidth of the radiation produced by the light source was adjusted about the normal operating point by altering the fluorine (F_2) concentration of the master oscillator (MO) gain medium and additionally by controlling the time delay between commutation of the MO and PA pulsed-power. These methods modulate the bandwidth because the spectrum of the MO output light is time-dependent, becoming narrower and narrower with each round trip through the line-narrowing elements of the laser resonator. The length of time the MO-laser stays above oscillation threshold depends on the gas pressure and F_2 concentration, so changes in the gas mixture can be used to alter the bandwidth of the output radiation. Similarly, the optical bandwidth of a MOPA-system output depends upon the time delay between the onset of laser oscillation in the MO and the appearance of gain in the power amplifier (PA) chamber because the PA can selectively amplify a portion of the MO pulse. Normally in the laser this time delay Δt_{MOPA} is automatically adjusted by a servomechanism to the value that maximizes the electrical-to-optical conversion efficiency of the system. By disabling this feedback and instead locking Δt_{MOPA} to a fixed value, we used the time-dependent PA gain as a temporal "gate" with which it was possible to select a wider- or narrower-bandwidth portion of the MO output pulse. The energy stability of the system was not compromised due to the high intrinsic stability of the laser pulsed-power generation. Because certain qualities of the output beam (i.e., divergence, amplified spontaneous emission, etc.) may depend on Δt_{MOPA} and MO F_2 enrichment as well, the performance of the output parameters of the laser against such timing variation was characterized at the factory and also, in some cases, *in situ* with the actual tool to ensure that those beam qualities parameters did not vary significantly.

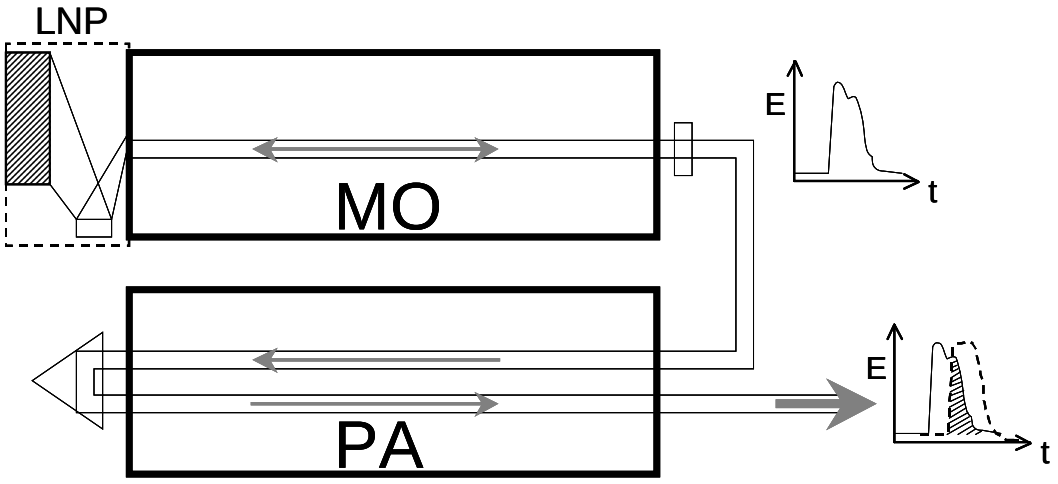

Figure 5.
XLA 140 MOPA architecture. MO=Master Oscillator, PA=Power Amplifier, LNP=Line-Narrowing Package. Inset graphs illustrate how temporal overlap of MO oscillation and PA gain can be used to selectively amplify only a portion of the MO pulse.

The bandwidth of illuminating radiation was continuously monitored during the experiment using a Cymer Bandwidth Analysis Module (BAM). The BAM is a second generation etalon spectrometer optimized to provide simultaneous measurement of spectral full width at half-maximum (FWHM) bandwidth and the bandwidth of the integrated energy containing 95% of the output (E_{95}). The BAM makes use of a number of special techniques to suppress systematic errors that degrade the usefulness of similar imaging etalon spectrometers, especially those terms that can make the readout dependent on the absolute operating wavelength or detailed shape of the light source spectrum[4]. With such special enhancements, etalon spectrometers can be made to indirectly infer (that is, without the need for deconvolution)

the light source bandwidth with a precision comparable to that of a state-of-the-art high-resolution Echelle grating spectrometer.

Prior to each exposure run, the operating point of the light source was adjusted to obtain the four bandwidth-setpoints listed in Table 2, and preparatory characterizations of the bandwidth and energy stability were made. Some of these points were well outside the normal operating range of the laser. During wafer exposures, the pulse-by-pulse streaming data functionality of the laser allowed bandwidth, energy-dose stability, and other data to be continuously collected. Therefore it was possible to make a 1:1 correlation between the measured bandwidth values and the pulses delivered to the exposure fields on the wafers. For purposes of analysis, the average bandwidth over each die was computed.

Table 2.
Experimental bandwidth settings.

Setting	E_{95} Bandwidth	FWHM Bandwidth
1	0.28 pm	0.12 pm
2	0.32 pm	0.13 pm
3	0.38 pm	0.14 pm
4	0.59 pm	0.18 pm

4 EXPERIMENTAL OPE-VS-BANDWIDTH RESULTS.

A Nikon S307E scanner was used to pattern high L-NA > 0.70 exposures of line CD through pitch as the E_{95} bandwidth was varied experimentally from 0.28 to 0.59 pm. The scanner was set to conditions given in Table 1, while *in situ* aerial image focus calibration was performed prior to the wafer exposure to ensure proper focusing. No statistical change in the system focus was detected during the duration of the experiment, which is as expected, as a narrowing or broadening of the spectral bandwidth does not change the center wavelength. 4 identical thin-film substrates coated with a line/space resist were exposed with an EPSM reticle containing a wide range of line features at the same width with different spacing, referred to as coherence combs. Each wafer was processed using the identical track modules to minimize track process variation. Coherence combs with line features of 80, 90, 100, 110, 130, 160, 280 and 320 nm through nested to isolated line pitch ranges of roughly 170 - 2300 nm (depending on the drawn line CD) were measured together using a single CD-SEM recipe. Six fields of identical conditions (bandwidth, exposure and focus) were measured on the CD-SEM and averaged at each bandwidth in order to accurately perceive statistical changes in CD as the bandwidth was varied. At each average E_{95} bandwidth setting, the variation in E_{95} during exposure of the measured die was minimal, with ranges of less than about 0.01 pm, according to *in situ* measurements. The CD data was analyzed in order to quantify the change in CD and the iso-dense bias, or OPE.

Shown in Figure 6 are the average 80 nm line OPE curves at each of the four bandwidth settings. Most of the line CDs decreased with increasing E_{95} bandwidth, indicative of a contrast loss, as expected. In Figure 7, the differences in the CDs have been plotted versus the drawn line/drawn space to help illustrate the observed CD changes with bandwidth. The y-axis error bars are computed as the RMSS of the standard deviation of the means (N = 6) of the CDs measured at E_{95} = 0.28 pm plus the standard deviation of the means (N = 6) at each of the other E_{95} settings given in Table 2. The isolated lines of L/S < 0.3 show the greatest rate of CD change with bandwidth, up to about −4 nm on average. The amount of CD variation with bandwidth decreases as the features become more nested and eventually become invariant to bandwidth at semi-nested pitches of around $0.8 \leq L/S \leq 0.9$. The pitch at which CD becomes invariant to bandwidth will depend on the mask and exposure bias used. In this case, at the densest pitches of L/S > 0.9, a slight increase in the nested line CD with increasing bandwidth is observed, although it is not statistically conclusive. The measured data can then be inserted into Equation 1 to compute the sensitivity parameter *S(p)* for the 80 nm line features and compared with the simulation results as shown in Figure 8.

The 80 nm line sensitivity parameter computed from the measured data, $S(p)_{meas}$, compares fairly well with the simulated results, $S(p)_{sim}$. Both show the same expected rate of CD loss with increasing E_{95} bandwidth of around −10 nm/pm for isolated lines. In the semi-isolated to semi-nested regime of $0.3 < L/S < 0.8$, both the experimental and simulated CD sensitivity to bandwidth exhibit the same lessening trend, although an offset between the two sensitivity parameters is evident. This is most likely due to a mismatch in the simulated aerial-image threshold and the actual resolution threshold of the resist, with the resist having a lower threshold than the one selected in the simulation. At the semi-nested pitches of around $0.8 \leq L/S \leq 0.9$, the experiment and model agree that the semi-nested line CDs become invariant to changing bandwidth. This unique condition of the semi-nested line results from the wide range of slopes of aerial images all sharing the same inflection point at precisely the resolution threshold. At this threshold, the slopes of the aerial images will decrease dramatically with defocus, however, the aerial images intersect each other at the same spatial position. Hence, the semi-nested line CD is invariant to bandwidth changes at this particular resolution threshold. At the tightest pitches of $L/S > 0.9$ for the 80 nm line, the $S(p)_{meas}$ and the $S(p)_{sim}$ both show a CD change *increase* with increasing E_{95} bandwidth of about 5 nm/pm. Unlike the semi-nested condition, the point at which the defocused aerial images share the same inflection point is below the resolution threshold. As the image is defocused, the aerial image above the resolution threshold broadens and decreases the amount of light entering toward the line center, resulting in a line CD increase.

The other OPE data collected in this experiment for the 90 nm lines and greater show similar trends and behavior, and hence are not reported for brevity.

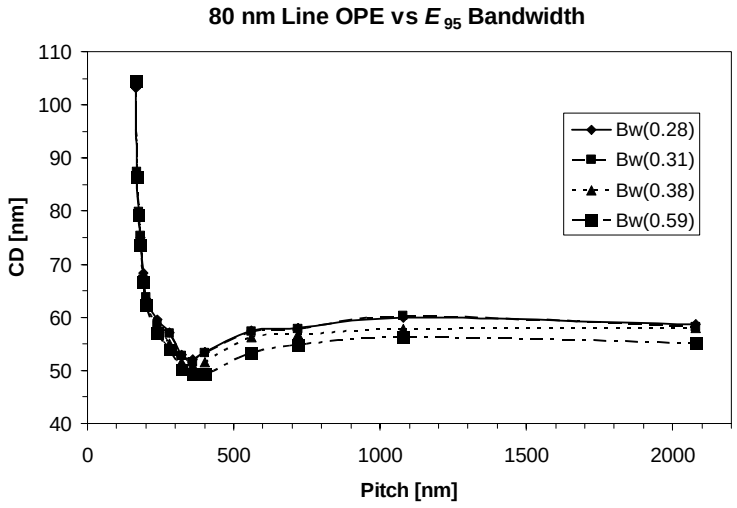

Figure 6.
The 80 nm line OPE curves as E_{95} bandwidth, showing a loss of contrast.

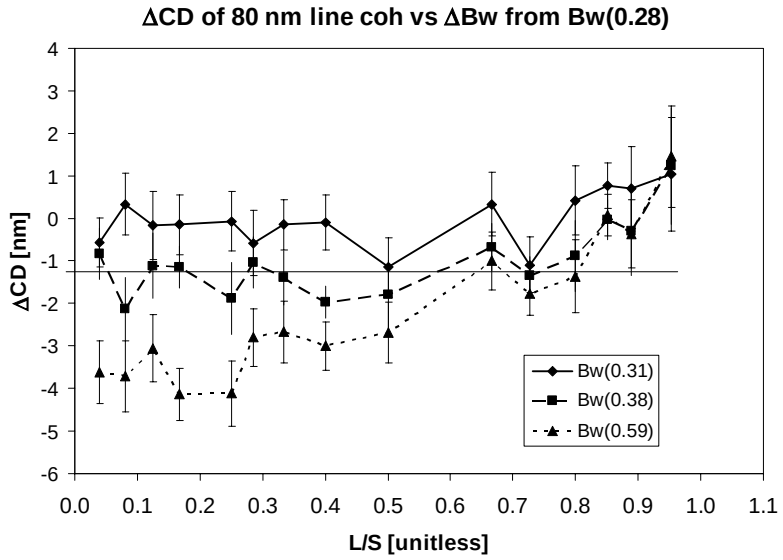

Figure 7.
The change in CDs from the E_{95} bandwidth = 0.28 pm. The x axis is plotted as drawn line/drawn space where isolated lines are found on the left, L/S < 0.3. The lines on the graph are drawn to guide the eye.

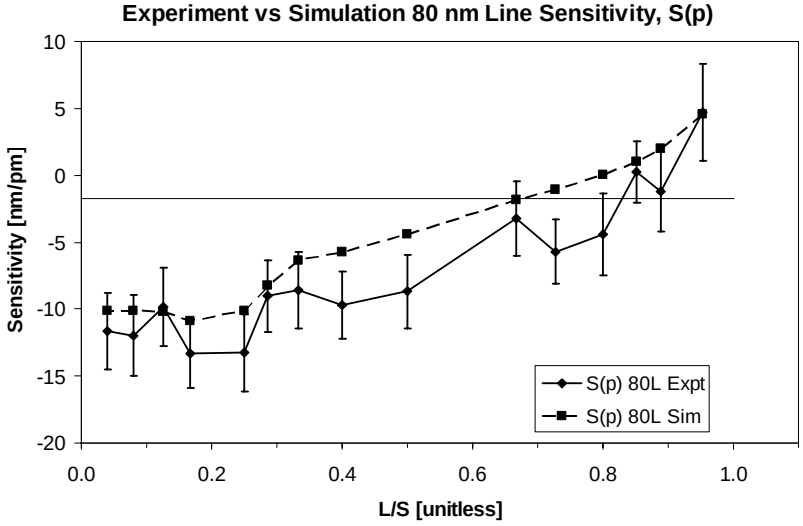

Figure 8.
A comparison of the measured and simulated 80 nm line sensitivity parameter. The lines on the graph are drawn to guide the eye.

5 DISCUSSION AND CONCLUSIONS.

Now that the sensitivity to bandwidth changes has been determined, and it has been seen that it can be modeled with reasonable accuracy, two questions must be answered:

- Since bandwidth is not perfectly stable over time, will drifting cause unexpected iso-dense bias shifts?
- How does this bandwidth effect compare to other changeable tool parameters?

The stability question is somewhat complicated to answer, since we have presented CD results vs. the E_{95} parameter, and current lasers generally report FWHM bandwidth, not E_{95}. From the lens manufacturer's point of view, E_{95} is a better performance predictor, but practical engineering issues have hitherto dictated the use of FWHM. Since the laser spectral shape is neither Gaussian not Lorentzian, and tends to change with laser conditions, we can *not* assume a constant ratio between the two bandwidth metrics, but we can approximate it. New developments in etalon-based spectroscopy have allowed highly accurate and reproducible measurement of both E_{95} and FWHM bandwidth which are insensitive to changes in spectral shape [5]. Such a module was used in this experiment and will be generally available to enhance the capability of future laser systems and as an upgrade for older systems.

In the meantime, one can estimate the likely drift in OPE as follows:

- Typical fab data for measured FWHM over time varies with a maximum range of about 0.06 pm (from 0.17 to 0.23 pm). From the data in Table 2, the E95/FWHM ratio is about 3.0 for this laser model. Hence E_{95} can be assumed to vary over a maximum range of about 0.18 pm under normal operating conditions. In fact, these ranges may be overestimates of the actual bandwidth variation during exposures, since the data include measurements under non-exposure conditions which are known to produce more extreme bandwidth changes.
- Isolated lines experienced a constant sensitivity of −10 nm/pm E_{95}, while the most sensitive dense lines increased +5 nm/pm E_{95}.

For an E_{95} range of 0.18 pm an estimated maximum of 2.7 nm (±0.5 nm) iso-dense bias drift may be expected. This is a significant amount of CD variation and indicates that additional bandwidth stabilization is necessary for critical layers. The expected performance of such stabilization concepts is described elsewhere[7].

There are, of course, other effects in the litho tool that can drive iso-dense bias or OPE changes. As reported[1,5] previously, it has been shown that primary OPE drivers on a scanner are, in rough order of importance, focus, dose, lens NA, and illuminator NA. Lens NA and illuminator NA have very similar effects. A sample of illuminator NA effects, from aerial-image modeling, is shown in Figure 9. The overall effect is similar to the bandwidth change, with isolated lines more strongly affected than dense lines, and with a smooth linear change as sigma is varied. Focus effects, not shown here, are similar except that the OPE shift is of course nonlinear with focus.

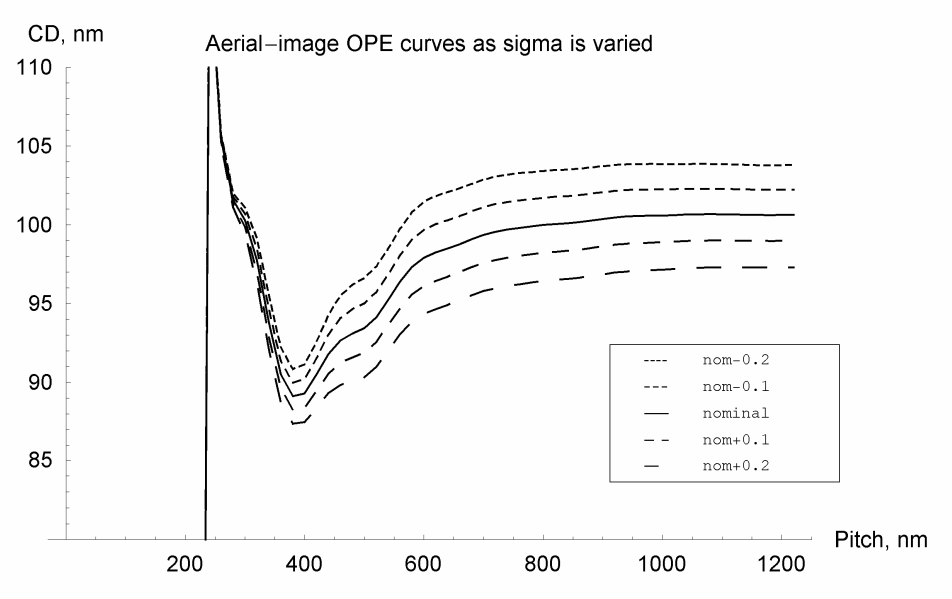

Figure 9.
Modeled OPE shifts due to detuning partial coherence from the nominal value.

Using that information, as well as experimental dose-sensitivity data, rough estimates of iso-dense bias shifts similar to those caused by bandwidth are shown in Table 3. “Isolated” means at a pitch of 1000 nm or greater, while “dense” refers to roughly equal lines and spaces. Broadly speaking, the focus and dose shifts cited in Table 3 are within the control limits of a modern lithographic scanner, while of course partial coherence does not tend to drift.

We see that the magnitude of the bandwidth effect is similar to those from other variables and is neither overwhelming nor negligible, but is indeed an additional control parameter to consider when attempting to control OPE behavior.

Table 3.
Roughly equal perturbers of iso-dense bias.
Exact values depend on the tool and on the process, so this is just a guide.

Approximately 1.0 nm iso-dense bias is caused by	
E_{95} bandwidth shift	0.1 pm
Focus shift	0.025 μ
Dose shift	0.4 mJ
Partial coherence shift	0.05

ACKNOWLEDGEMENTS

The authors would like to thank N. Tokuda and S. Slonaker for valuable discussions.

REFERENCES

[1] S.P. Renwick, "What makes a coherence curve change?", *Optical Microlithography XVIII*, B.W. Smith, ed., *Proceedings of SPIE* **5754**, p. 1537 -- 1547, SPIE, Santa Clara, 2005.

[2] D. Williamson, Nikon Research Corp. of America, private communication.

[3] "Behavior of lens aberrations as a function of wavelength on KrF and ArF lithography scanners," M. Terry, I. Lalovic, G. Wells, and A. Smith, *Optical Microlithography XIV*, C.J. Progler, ed., *Proceedings of SPIE* **4346**, p. 15 -- 24, SPIE, Santa Clara, 2001

[4] R.J.Rafac "Overcoming limitations of etalon spectrometers used for spectral metrology of DUV excimer light sources." *Optical Microlithography XVII*, B.W. Smith, ed., Proc. SPIE **5377** p. 846-858, 2004.

[5] S. P. Renwick, "Scanner parameters and OPE variation," presented at FujiFilm INTERFACE conference, San Diego, Sept. 2005; to be published.

7 W. J. Dunstan, R. Jacques, R.J. Rafac, R. Rao, F. Trintchouk, "Active Spectral Control of DUV light sources for OPE minimization", to be published at SPIE Optical Microlithography 2006